INTERNATIONAL JOURNAL FOR NUMERICAL AND ANALYTICAL METHODS IN GEOMECHANICS
*Int. J. Numer. Anal. Meth. Geomech.*, **23**, 1655–1674 (1999)

# WATER WAVE DRIVEN SEEPAGE IN SEDIMENT AND PARAMETER INVERSION BASED ON PORE PRESSURE DATA

YONGKE MU[1,*], ALEXANDER H-D. CHENG[1], MOHSEN BADIEY[2] AND RICHARD BENNETT[3]

[1]*Department of Civil and Environmental Engineering, University of Delaware, Newark, DE 19716, U.S.A.*
[2]*Graduate College of Marine Studies, University of Delaware, Newark, DE 19716, U.S.A.*
[3]*Seaprobe Inc., 501 Pine Street, Picayune, MS 39466, U.S.A.*

## SUMMARY

Water wave over a porous sea bottom drives a seepage flux into and out of the sediment. The volume of fluid exchange per wave cycle and per wave length may be tied to the mass transfer rate of contaminant in sediment. In the first part of the paper, the analytical solution of seepage flux is presented based on the Biot theory of poroelasticity. Parameter effect on the seepage flux as well as on the pore pressure is examined. In the second part, empirical relationships are introduced to reduce the data requirement of the model to two parameters: the porosity and the degree of saturation. With the existence of a multi-sensor piezometer known as 'MPAS', the pore pressure data in the sediment can be collected. Utilizing the empirical relations, parameter inversion can be achieved based on pore pressure data alone. Copyright © 1999 John Wiley & Sons, Ltd.

KEY WORDS: poroelastic; Water wave; Pore pressure; Seepage; Inversion

## 1. INTRODUCTION

Sediment in bays, estuaries, and in ocean near river outlets is often contaminated. Many inorganic contaminants, most notably heavy metals, do not decompose. These accumulated substances are released back into the receiving body of water through bottom mass transfer. The mass transfer rate is largely controlled by the seepage flux exchange between the sediment and the sea water. Larger wave action and higher sediment hydraulic conductivity generally cause larger transfer rate. The information of mass transfer rate is important in water quality modelling.

Water wave effects on the shallow sea sediment have been investigated by a number of investigators in the last few decades. Most of the earlier studies[1–5] assumed that the porous seabed was non-deformable. Some of the work also assumed that the pore water was incompressible. Madsen,[6] Yamamoto,[7] Mei and Foda[8] studied the sediment response based on the more rigorous Biot theory which takes into account the elastic deformation and the compressibility of pore water. These studies focused on the responses of pore water pressure, sediment stress, and deformation. Information concerning seepage flux, particular in the context of contaminant transport, was not given.

* Correspondence to: Yongke Mu, The Graduate College of Marine Studies, Robinson Hall, University of Delaware, Newark, DE 19716-3501, U.S.A.

Contract/grant sponsor: Office of Naval Research

CCC 0363–9061/99/131655–20$17.50

*Received 18 November 1998*
*Revised 5 February 1999*

In the present paper we study the problem of a water wave propagating over a porous sediment. The pressure variation at the sea bottom due to the wave motion drives a seepage flow into and out of the sediment. As both the fluid and the porous solid skeleton are deformable, the coupled poroelasticity theory of Biot[9] is used. The parameter effects on the pore water pressure and on the seepage flux are studied. A difficulty in using the Biot model for practical application is that it requires a large number of physical parameters as input. Direct measurement of these parameters is not practical due to the relative inaccessibility of the seabed and the difficulty in extracting intact samples. The existence of a technology of measuring *in situ* pore pressure data using an instrument known as 'MPAS'[10] offers an opportunity to determine parameters by inverse method. The success of an inverse method however is dependent on the sensitivity of the response signal (e.g. pore pressure) to the parameter variation. It is in fact not possible to determine all the parameters by the pore pressure data alone. A certain break through is needed.

Prior field and laboratory measurements have established that there exist certain relations among the sediment parameters. By a compilation of these relations, Badiey *et al.*,[11] proposed a model that allows the reduction of the number of input parameters needed for the Biot model. It was demonstrated that only two parameters, the porosity and the degree of saturation, are required, under the condition of a lack of direct measurement.

In this paper, the sensitivity of pore pressure response to the variation of the porosity and the degree of saturation is demonstrated. An inverse method is designed to find these parameters based on *in situ* pore pressure data.

## 2. GOVERNING EQUATIONS

Assume a linear, sinusoidal water wave propagating over sea bottom sediment with water depth $h_2$. The geometry of the two-dimensional problem is illustrated in Figure 1. The $x$-axis is in the wave propagating direction, parallel to the sediment surface, and the $z$-axis is chosen to be vertically downward from the sea-seabed interface. The Biot[9] model, which takes into account the

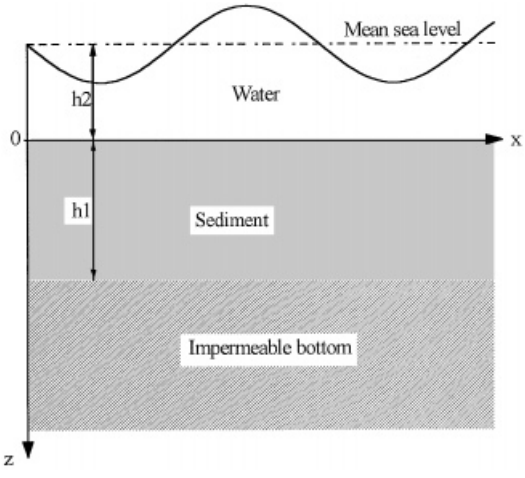


Figure 1. Geometric sketch of the environmental conditions in shallow water

 

compressibility of pore water and the porous media is adopted. Since the governing equations are linear, we can follow the customary approach of removing the hydrostatic components of pore water pressure, stresses and strains in the sediment. Only the incremental components of such variables are considered, unless otherwise mentioned.

The pore pressure is governed by an anisotropic diffusion equation in a homogeneous media as[9,12]

$$k_x \frac{\partial^2 p}{\partial x^2} + k_z \frac{\partial^2 p}{\partial z^2} = \frac{\gamma_w}{M} \frac{\partial p}{\partial t} + \gamma_w \alpha \frac{\partial \varepsilon}{\partial t} \tag{1}$$

where $p$ is the wave induced pore water pressure; $k_x$, $k_z$ are the principle hydraulic conductivities in $x$ and $z$ directions; $\gamma_w$ is the specific weight of pore water, $\gamma_w = \rho_w g$; $\alpha$ is the Biot effective stress coefficient which can be calculated from

$$\alpha = 1 - K/K_s \tag{2}$$

and $M$ is the Biot modulus which is defined as:[12]

$$\frac{1}{M} = \frac{K}{K_s}\left(\frac{1}{K} - \frac{1}{K_s}\right) + \phi\left(\frac{1}{K_f} - \frac{1}{K_s}\right) \tag{3}$$

and

$$\frac{1}{K_f} = \frac{1}{K_w} + \frac{1 - S_r}{P_0} \tag{4}$$

in the above $\phi$ is the porosity of sediment, $K_s$ is the bulk modulus of the solid grain, $K$ is the bulk modulus of the skeleton frame, $K_f$ is the apparent bulk modulus of water, $K_w$ is the true bulk modulus of water, $S_r$ is the degree of saturation and $P_0$ is the average absolute pore water pressure in the sediment. The volumetric strain $\varepsilon$ for two-dimensional problem is

$$\varepsilon = \partial u/\partial x + \partial w/\partial z \tag{5}$$

where $u$, $w$ are the $x$ and $z$ components of solid frame displacements, respectively.

Using the effective stress concept, the force equilibrium of a porous medium sample is given by[9,12]

$$\partial \sigma_x/\partial x + \partial \tau/\partial z = \alpha(\partial P/\partial x) \tag{6}$$

$$\partial \sigma_z/\partial z + \partial \tau/\partial x = \alpha(\partial p/\partial z) \tag{7}$$

where $\sigma_x$, $\sigma_z$, $\tau$ are wave induced effective normal and shear stress. Here the elasticity convention, namely that tensile stress is denoted positive, is adopted. The Hooke's law is applied to the effective stresses such that

$$\sigma_x = \frac{2G(1-v)}{1-2v}\left[\frac{\partial u}{\partial x} + \frac{v}{1-v}\frac{\partial w}{\partial z}\right] \tag{8}$$

$$\sigma_z = \frac{2G(1-v)}{1-2v}\left[\frac{\partial w}{\partial z} + \frac{v}{1-v}\frac{\partial u}{\partial x}\right] \tag{9}$$

$$\tau = G\left[\frac{\partial u}{\partial z} + \frac{\partial w}{\partial x}\right] \tag{10}$$

in the above, $G$ is the shear modulus and $v$ is the Poisson ratio.

 

## 3. GENERAL SOLUTION

Equations (8)–(10) can be used to eliminate the stresses in equations (6) and (7). The three equations (1), (6) and (7) can be used to solve for the three unknowns $w$, $u$, and $p$.

To define the problem, boundary conditions are needed. At the sediment surface, the boundary conditions are prescribed based on the sea bottom pressure exerted by a travelling water wave. The pore pressure is the same as the water pressure in the water column, and the effective stress is the difference between the total stress (equal to water pressure) and the pore pressure modified by the effective stress coefficient. The shear stress is zero as the water wave is considered inviscid.[4,6–8,12] These boundary conditions can be summarized as follows:

$$\sigma_z = \mathrm{Re}\{(\alpha - 1)p_0 \exp[\mathrm{i}(\omega t + \lambda x)]\} \tag{11}$$

$$\tau = 0 \tag{12}$$

$$p = \mathrm{Re}\{p_0 \exp[\mathrm{i}(\omega t + \lambda x)]\} \tag{13}$$

in the above, we have used the complex variable representation for the sinusoidal water wave in order to simplify the mathematics. We note that $\mathrm{i} = \sqrt{-1}$, $p_0$ is the pressure at the sediment surface, which, according to linear water wave theory, can be given by,

$$p_0 = (\gamma_w H/2)/\cosh \lambda h_2 \tag{14}$$

in which $H$ is the water wave height, $\lambda$ is the wave number and $\omega$ is the water wave angular frequency. In reality, this pressure is measured directly by a transducer positioned at the mud line.

For a sea bed with an impermeable rigid bottom at a depth $z = d$, the boundary conditions are that no sediment displacement and no fluid flow across the boundary are allowed, i.e.

$$u(d) = 0 \tag{15}$$

$$w(d) = 0 \tag{16}$$

$$\partial p(d)/\partial z = 0 \tag{17}$$

In the case of a semi-infinite sediment, the boundary conditions are given at infinity as

$$u, w, p \to 0 \qquad \text{as } z \to \infty \tag{18}$$

Since the boundary conditions (11) and (13) are periodic in both time and space, there exists a corresponding periodic solution of

$$u = U(z) \exp[\mathrm{i}(\omega t + \lambda x)] \tag{19}$$

$$w = W(z) \exp[\mathrm{i}(\omega t + \lambda x)] \tag{20}$$

$$p = P(z) \exp[\mathrm{i}(\omega t + \lambda x)] \tag{21}$$

in which $U$, $W$, $P$ are functions of $z$ only. The above variables are all extended to complex variables. But only the real parts of $u$, $w$, $p$ carry physical meanings.

 

The general solutions of $U$, $W$, $P$ can be found as[6, 7, 13]

$$U(z) = \mathrm{i}p_0[a_1\sinh(\lambda z) + a_2 z\sinh(\lambda z) + a_3\cosh(\lambda z) + a_4 z\cosh(\lambda z) + a_5\sinh(\lambda' z) + a_6\cosh(\lambda' z)] \tag{22}$$

$$W(z) = \mathrm{i}p_0[b_1\sinh(\lambda z) + b_2 z\sinh(\lambda z) + b_3\cosh(\lambda z) + b_4 z\cosh(\lambda z) + b_5\sinh(\lambda' z) + b_6\cosh(\lambda' z)] \tag{23}$$

$$P(z) = \mathrm{i}p_0[c_1\sinh(\lambda z) + c_2 z\sinh(\lambda z) + c_3\cosh(\lambda z) + c_4 z\cosh(\lambda z) + c_5\sinh(\lambda' z) + c_6\cosh(\lambda' z)] \tag{24}$$

in which

$$\lambda' = \lambda \cdot \lambda_* \tag{25}$$

$$\lambda_*^2 = k_x/k_z + \theta^2/\lambda^2 \tag{26}$$

$$\theta^2 = (\mathrm{i}\omega\gamma_w\alpha/k_z)\left[\frac{1}{M\alpha} + \frac{\alpha(1-2v)}{2G(1-v)}\right] \tag{27}$$

The constants $a_i, b_i, c_i$ $(i = 1, 2, \ldots, 6)$ can be determined from equations (1)–(10) with the proper boundary conditions. Substitution of (22)–(24) into equations (1)–(10) gives the following relations:

$$\begin{aligned}
&b_1 = -\mathrm{i}a_3 + \mathrm{i}A_1 a_2, && b_2 = -\mathrm{i}a_4\\
&b_3 = -\mathrm{i}a_1 + \mathrm{i}A_1 a_4, && b_4 = -\mathrm{i}a_2\\
&b_5 = -\mathrm{i}\lambda_* a_6, && b_6 = -\mathrm{i}\lambda_* a_5\\
&c_1 = -\mathrm{i}A_2 a_4, && c_2 = 0\\
&c_3 = -\mathrm{i}A_2 a_2, && c_4 = 0\\
&c_5 = \mathrm{i}A_3 a_5, && c_6 = \mathrm{i}A_3 a_6
\end{aligned} \tag{28}$$

where

$$A_1 = \frac{1}{\lambda}\frac{\alpha + \frac{3-4v}{1-2v}\left[\frac{G}{\alpha M} - i(k_z - k_x)\frac{\lambda^2 G}{\alpha\omega\gamma_w}\right]}{\alpha + \frac{1}{1-2v}\left[\frac{G}{\alpha M} - i(k_z - k_x)\frac{\lambda^2 G}{\alpha\omega\gamma_w}\right]} \tag{29}$$

$$A_2 = \frac{2G}{\alpha + \frac{1}{1-2v}\left[\frac{G}{\alpha M} - i(k_z - k_x)\frac{\lambda^2 G}{\alpha\omega\gamma_w}\right]} \tag{30}$$

$$A_3 = \frac{2KG(1-v)}{\alpha(1-2v)}(1 - \lambda_*^2) \tag{31}$$

 

The remaining six coefficients ($a_1$–$a_6$) are determined from six boundary conditions. Three of which are given at the sea-sediment interface, as described in equations (11)–(13), and others are given by the basement assumptions. For example, for sediment overlaying an impermeable basement case, conditions (15)–(17) are satisfied, and a $6 \times 6$ matrix equation system can be constructed by substituting (22)–(24) to the boundary conditions. The unknowns $a_i$ ($i = 1, 2, \ldots, 6$) can be solved analytically (see Appendix, Case 1).

The pore pressure is then obtained as

$$p(z) = p_0 A_2 \left[ a_4 \sinh(\lambda z) + a_2 \cosh(\lambda z) - \frac{A_3}{A_2} a_5 \sinh(\lambda' z) - \frac{A_3}{A_2} a_6 \cosh(\lambda' z) \right] \cdot e^{i(\omega t + \lambda x)} \tag{32}$$

In case of semi-infinite sediment, conditions in (18) are satisfied. The solution of the system is (See Appendix, Case 2):

$$a_1 = \frac{A_1 C_2 - A_1 C_1 c'}{2 A_2 C_2} + \frac{\lambda_* C_1 c'}{A_3 C_2} \tag{33}$$

$$a_2 = \frac{C_2 - C_1 c'}{A_2 C_2} \tag{34}$$

$$a_5 = \frac{C_1 c'}{A_3 C_2} \tag{35}$$

Hence, a simpler analytical expression of the pore pressure $p$ is obtained, which can be explicitly expressed as

$$p(z) = p_0 \left[ \left( 1 - \frac{C_1 c'}{C_2} \right) e^{-\lambda z} + \frac{C_1 c'}{C_2} e^{-\lambda' z} \right] \cdot e^{i(\omega t + \lambda x)} \tag{36}$$

where

$$C_1 = \alpha + m - 1 \tag{37}$$

$$C_2 = \lambda_* + (\alpha + m) c' - 1 \tag{38}$$

$$m = \frac{1}{1 - 2\nu} \left[ \frac{G}{\alpha M} - i(k_z - k_x) \frac{\lambda^2 G}{\alpha \omega \gamma_w} \right] \tag{39}$$

$$\lambda_*^2 = \frac{k_x}{k_z} + \frac{D}{k_z} \tag{40}$$

$$D = \frac{i \omega \gamma_w \alpha}{\lambda^2} \left( \frac{1}{\alpha M} + \frac{\eta}{G} \right) \tag{41}$$

$$c' = \frac{1}{2\eta} (1 - \lambda_*^2) \tag{42}$$

$$\eta = \frac{\alpha (1 - 2\nu)}{2(1 - \nu)} \tag{43}$$

 

With the condition of $K_s \gg K$, hence $\alpha \approx 1$, and $1/M \approx \beta\phi$, where $\beta$ is the apparent pore water compressibility, the above result reduces to that of Madsen.[6] If we further assume $k_x = k_z$, the result is that of Yamamoto.[7] In this case the pore pressure can be simplified to

$$p(z) = p_0 \frac{\eta - 1 + m e^{-i\omega\gamma(M+\eta)z/\lambda}}{\eta - 1 + m} e^{-\lambda z} e^{i(\omega t + \lambda x)} \tag{44}$$

## 4. SEEPAGE FLUX

In this section, the volume of seepage exchange between the sea and sea bottom driven by the water waves is studied. It is an important step toward studying the water pollution in coastal areas.

The net seepage flux over one wave length at any instant or over one wave period at any fixed point is zero. However, for the purpose of mass transport caused by the cyclic wave motion, the relevant quantity is the volume of water pumped in or out over one-half wave period ($T$) and one-half wave length ($L$). This volume (per unit width of sea bottom) is first expressed as a function of depth $z$:

$$V(z) = -\int_{-T/4}^{T/4} \int_{-L/4}^{L/4} \frac{k_z}{\gamma_w} \frac{\partial p}{\partial z} \mathrm{d}x\, \mathrm{d}t \tag{45}$$

For sediment with an impermeable rigid bottom, we have, after integration,

$$V(z) = \frac{4k_z p_0 A_2}{\omega\gamma_w} \left[ a_4 \sinh(\lambda z) + a_2 \cosh(\lambda z) - \frac{A_3}{A_2} a_5 \sinh(\lambda' z) - \frac{A_3}{A_2} a_6 \cosh(\lambda' z) \right] \tag{46}$$

For semi-infinite sediments, the integration of (45) gives

$$V(z) = \frac{4k_z p_0}{\omega\gamma_w} \left[ \left( 1 - \frac{C_1 c'}{C_2} \right) e^{-\lambda z} + \frac{C_1 \lambda_* c'}{C_2} e^{-\lambda' z} \right] \tag{47}$$

As an example we focus on the semi-infinite sediment problem. At water and sediment interface, $z = 0$, we have

$$\begin{aligned} V_0 &= V(0) \\ &= \frac{4k_z p_0}{\omega\gamma_w} \left[ 1 + (\lambda_* - 1) \frac{C_1 c'}{C_2} \right] \end{aligned} \tag{48}$$

where $V_0$ is the volume of water exchanged with the ocean per unit width of sea bed in the $y$-direction. In the case of $\alpha = 1$ and $k_x = k_z$, the seepage exchange (48) reduces to

$$V_0 = \frac{4k_z p_0}{\omega\gamma_w} \left( 1 + \frac{(\lambda_* - 1) m c'}{\lambda_* - 1 + (1 + m) c'} \right) \tag{49}$$

For a fully saturated sediment, the compressibility $\beta$ is given by $1/K_w$ with $K_w = 2{\cdot}0 \times 10^9$ Pa. We note that the shear modulus $G$ varies from $5{\cdot}0 \times 10^5$ to $5{\cdot}0 \times 10^8$ Pa for a wide range of sediments.

 

Hence $G\beta = G/K_w$ is a small number for most sediments except for dense sand which has a higher $G$ value. The volume exchange (48) may be approximated as $V_a$ given by

$$V_a = (4k_z/\omega\gamma_w)p_0 \tag{50}$$

which shows a linear relationship to the hydraulic conductivity. This result can also be derived from the assumption of rigid soil and incompressible pore fluid.

In reality, the sea sediment is not completely saturated. Practically, the decomposition of organic materials often generate methane bubbles in the pore water. Since our interest lies in the pollution of estuary and near shore water, the existence of gas in the sediment is common. When pore water is not completely saturated, the compressibility of water drastically increases. It generally increases flux into the sediment. We shall examine this effect in the next section.

## 5. PARAMETER ANALYSIS

Due to the relatively large number of parameters involved in Biot's model, a full range parameter study is not desirable. We are also aware that in practical situations, it is rare that all these parameters are available from direct measurement. Limiting our attention to ocean sediments and utilizing the knowledge of empirical relations accumulated in this field, a simpler version of the model emerges. We notice that the solid grain bulk modulus ($K_s$), the grain bulk density ($\rho_s$), the water bulk modulus ($K_w$) and its density ($\rho_w$) are relatively constant. Hence the required parameters reduce to the frame bulk modulus ($K$), the shear modulus ($G$), the permeability ($k$), the porosity ($\phi$) and the degree of saturation ($S_r$). However, relative inaccessibility of the sediment material makes the direct measurement of these physical parameters difficult. Therefore, empirical relationships are introduced and used in many practical problems.

Porosity is a parameter that is relatively easy to obtain. For example, it can be calculated by the bulk density of a core sample, given the grain and water density. Hence, the statistical relationship between porosity and other parameters have been studied by many researchers.[11,14,15]

A relationship between shear modulus and porosity was studied by Yamamoto *et al.*[15] and reexamined by Badiey *et al.*[11] which is given as follows:

$$G = \alpha_1 \left[\frac{1-\phi}{\phi}\right]^{\alpha_2} \sigma_0^{1/2} \tag{51}$$

in the above, $G$ is in unit of Pascal (Pa), $\sigma_0$ is the average effective confining pressure defined by

$$\sigma_0 = \frac{1}{3} g(1 + 2K_0)(\rho_s - \rho_w) \int_0^z [1 - \phi(z)]\, dz \tag{52}$$

where $g$ is the gravitational acceleration, and $K_0$ is the coefficient of earth pressure at rest, which is 0·5 for most marine sediments.[16] $\alpha_1$ and $\alpha_2$ are empirical constants, depending on different sediment materials. For example, $\alpha_1 = 2{\cdot}44 \times 10^5$ and $\alpha_2 = 1{\cdot}628$ were found for sand-clay mixtures based on data collected from Atlantic Generation Station (AGS) and other sites.[11] Considering the porosity as constant with 1 m over burden pressure, equation (52) may be written as

$$G = 103{\cdot}1\,\alpha_1 \frac{(1-\phi)^{\alpha_2 + 0{\cdot}5}}{\phi^{\alpha_2}} \tag{53}$$

 

The empirical relationship between the frame bulk modulus and the porosity can be written as

$$K = a_1 \exp(-a_2\phi)(\text{Pa}) \tag{54}$$

Hamilton[17] suggested that

$$a_1 = 5{\cdot}121 \times 10^{10} \quad \text{and} \quad a_2 = 9{\cdot}795, \quad \text{Natural marine sands} \tag{55}$$

$$a_1 = 5{\cdot}443 \times 10^{10} \quad \text{and} \quad a_2 = 9{\cdot}788, \quad \text{Natural silty clay} \tag{56}$$

The experimental data used by Hamilton are referred to the equivalent of 1 m or less of over burden pressure.

The intrinsic permeability can be estimated from the porosity by the Kozeny–Carman equation:[14]

$$\kappa = \phi^3/CS_0^2(1-\phi)^2 \tag{57}$$

in which, $S_0 = 6/d_m$ is the specific surface of solid material, $d_m$ is the mean grain diameter, and $C$ is an empirical constant. $C \approx 5$ is good for sandy sediments. The hydraulic conductivity is then expressed as

$$k = (\gamma_w/\mu)\kappa \tag{58}$$

With these empirical relations, only the porosity, degree of saturation and the mean grain diameter will be needed for the theory. Assuming that we also have some knowledge about mean grain size diameter based on the types of sediment under investigation, only two parameters are needed in the full Biot model. The empirical relations provide a minimum requirement of physical parameters. Without further information available, these empirical relations will be used for the prediction of the seepage flux.

In the following, we examine the proposed theory by a numerical example. We choose the basic parameters as: $(K_w, K_s, \phi, S_r, d_m, \rho_s, \rho_w) = (2{\cdot}0 \times 10^9 \text{ Pa}, 3{\cdot}6 \times 10^{10} \text{ Pa}, 0{\cdot}4, 0{\cdot}99, 1{\cdot}65 \times 10^{-4} \text{ m}, 2650 \text{ kg/m}^3, 1025 \text{ kg/m}^3)$. With mean grain diameter of 164 μm, the permeability, the bulk modulus and the shear modulus are $2{\cdot}61 \times 10^{-4}$ m/s, $1{\cdot}02 \times 10^9$ (Pa) and $3{\cdot}77 \times 10^7$ (Pa), respectively.[18] The parameters related to the water wave are: water wave period $T = 6$ s, wave length $L = 10$ m, wave height $H = 1{\cdot}5$ m, and water depth $d = 15$ m.

At the degree of saturation less than 100 per cent, the assumption of $G\beta$ being small is no longer valid. Equation (48) or (49) should be used to evaluate the flux. For this example, the seepage exchange at the ocean-sediment interface is

$$V_0 = 1{\cdot}68\, V_a.$$

where $V_a = 4k_z p_0/(\omega\gamma_w)$, as evaluated from equation (50).

Considering an area of 100 m × 100 m, in a period of 24 h the volume of seepage exchanged is approximately 150 m$^3$ for this example.

Next, we take into account the uncertainty of the porosity and assume that $\phi$ is normally distributed with a standard deviation $\sigma_\phi = 25$ per cent of $\phi$. A stochastic analysis on parameter $\phi$ is conducted.[19,20] The mean seepage flux ratio at the sea–sediment interface is obtained as $\overline{(V_0/V_a)} = 1{\cdot}86$, and its standard deviation is $\sigma_{V_0/V_a} = 0{\cdot}71$. To view the flux ratio variation with

 

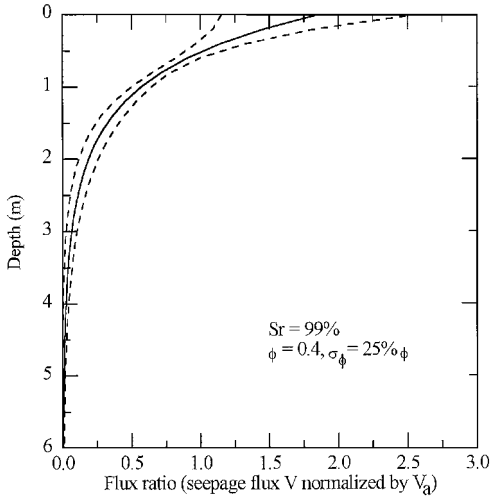


Figure 2. Flux ratio (seepage flux $V$ normalized by $V_a$) distribution versus depth with $\pm$ one standard deviation envolopes

sediment depth, in Figure 2, the distribution of flux ratio which is $V(z)$ from equation (47) normalized by $V_a$ is plotted versus depth. The one standard deviation envelopes are also presented in the plot. Note that the flux ratio rapidly decreases with depth. Since $V_a$ is depth independent, the rapid decrease of the flux ratio is due to the depth dependence of the seepage flux $V(z)$.

Figure 3 shows a contour plot of the flux ratio (seepage flux $V_0$ normalized by $V_a$) at the water—sediment interface as a function of porosity and degree of saturation. It is found that the flux ratio is strongly dependent on the porosity for lower degree of saturations. With the increase of the degree of saturation, the flux ratio generally decreases. For the fully or near fully saturated sediment, the flux ratio is almost equal to one, hence the approximation $V_a$ is accurate. For a sediment that has relatively lower degree of saturation, formula (48) or (49) should be used.

From Figure 3, we also conclude that, at a given porosity, the seepage flux increases with the degree of saturation decreasing. This is due to the fact that under-saturation increases the pore pressure gradient, but the permeability keeps unchanged. For a given degree of saturation, the flux ratio increases as the porosity decreases. The seepage flux, in this case, generally decreases, since the hydraulic conductivity decreases drastically. For example, for porosity from 0·5 to 0·25 with grain size 165 μm, the hydraulic conductivity varies from $0{\cdot}742 \times 10^{-4}$ to $0{\cdot}412 \times 10^{-5}$ m/s. In Figure 4 the normalized pore pressure and its phase lag are plotted versus depth at two different porosities. It is clear that, for low porosities, the amplitude decreases faster. In this example the amplitude of the pore pressure reduces to almost zero after 4 m. The phase lag of the pore pressure increases for lower porosities. This phenomena generally causes a big variation of the flux ratio.

Recognizing that the water wave frequency may differ from time to time (e.g. different weather conditions), the wave frequency effect on the seepage exchange is analysed. We keep all the parameters unchanged except the wave frequency. In Figure 5, we present the seepage flux ratio at the sea–sediment interface versus wave frequencies. It clearly shows that variation of the flux

 

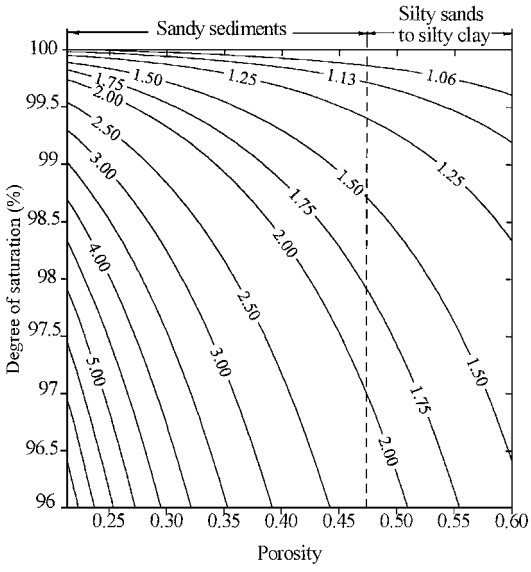


Figure 3. Contour of the flux ratio ($V_0/V_a$) as a function of porosity and degree of saturation at the sea–sediment interface

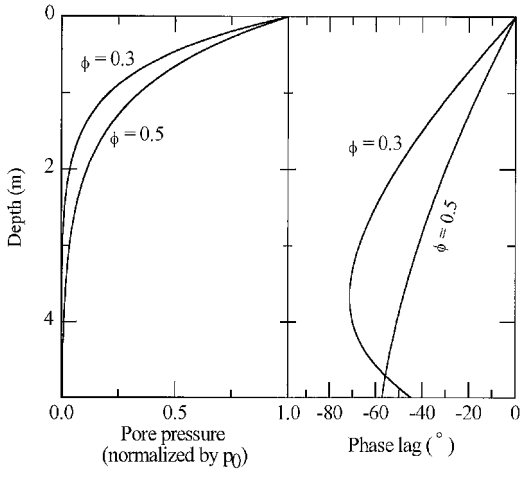


Figure 4. Pore pressure and its phase lag variation with sediment depth

ratio strongly depends on the saturation level. Generally, with frequency tends to zero, the flux ratio tends to unity, which means that the Darcy's law provides a good approximation of the seepage flux under assumption of only wave frequency varying. Practically, since the wave length and the wave numbers may also change with the frequency, further studies are needed for best understanding of the wave frequency effect on the seepage flux. This analysis may provide important information for the study of water quality contol in estuaries.

 

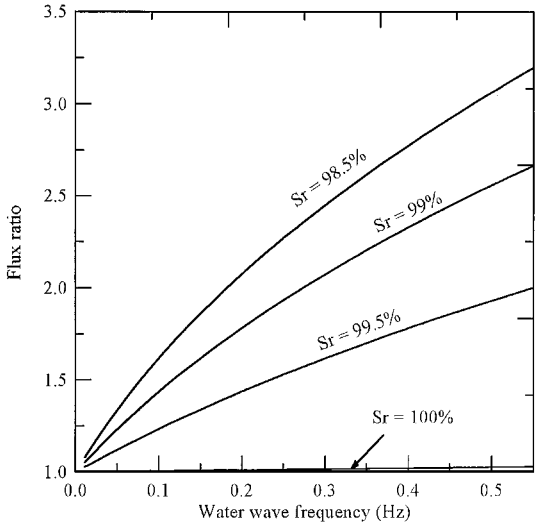


Figure 5. Water wave frequency effect on the seepage flux ratio. Curves are plotted in different degree of saturations

## 6. PORE PRESSURE SENSITIVITY ANALYSIS

With the introduction of the empirical relations, the actual physical parameters used for the forward model reduce to only two, the porosity and the degree of saturation. These two parameters are generally not available and need to be determined either from *in situ* measurements or from inversion techniques. Instead of direct measurement of these parameters, the pore pressure and its phase lag may be easily measured, and the porosity and the degree of saturation may be inverted from the data. However, the sensitivity of the pore pressure to the variation in porosity and the degree of saturation need to be examined first.

The pore pressure sensitivity to parameters is defined by taking the derivatives of the pressure with respect to that parameter. Considering a homogeneous and isotropic medium, we let $k_x = k_z = k$. The derivative of the pore pressure (equation (36)) with respect to the porosity and the degree of saturation are:

$$\frac{\partial p}{\partial \phi} = \frac{\partial p}{\partial M^{-1}} \frac{\partial M^{-1}}{\partial \phi} + \frac{\partial p}{\partial G} \frac{\partial G}{\partial \phi} + \frac{\partial p}{\partial k} \frac{\partial k}{\partial \phi} + \frac{\partial p}{\partial \phi} \tag{59}$$

$$\frac{\partial p}{\partial S_r} = \frac{\partial p}{\partial M^{-1}} \frac{\partial M^{-1}}{\partial S_r} = -\frac{\phi}{P_0} \frac{\partial p}{\partial M^{-1}} \tag{60}$$

where

$$\frac{\partial p}{\partial k} = p_0 \left\{ \frac{C_1 b^2 c'}{2k\lambda_* C_2^2} e^{-\lambda z} + \left[ \frac{z\lambda b(b+2) C_1 c'}{2k\lambda_* C_2} - \frac{C_1 b^2 c'}{2k\lambda_* C_2^2} \right] e^{-\lambda' z} \right\} e^{i(\omega t + \lambda x)} \tag{61}$$

$$\frac{\partial p}{\partial M^{-1}} = p_0 \left[ \left( \frac{B_1 C_3 - B_2 C_1}{C_2^2} - \frac{C_1 c'}{C_2} \frac{i\omega\gamma_w z}{2k\lambda'} \right) e^{-\lambda' z} - \frac{B_1 C_3 - B_2 C_1}{C_2^2} e^{-\lambda z} \right] e^{i(\omega t + \lambda x)} \tag{62}$$

 

$$\frac{\partial p}{\partial G} = p_0 \left[ \frac{mC_3 c' + B_3 C_1 (b + c'\eta/\lambda_*)}{GC_2^2} (e^{-\lambda' z} - e^{-\lambda z}) + \frac{C_1 z \lambda \eta B_3 c'}{\lambda_* G C_2} e^{-\lambda' z} \right] e^{i(\omega t + \lambda x)} \tag{63}$$

where

$$B_1 = Gc'/(1 - 2v)\alpha \tag{64}$$

$$B_2 = \frac{i\omega\gamma_w}{2k\eta\lambda^2}(b + \eta c'/\lambda_*) \tag{65}$$

$$B_3 = \frac{1}{2K_z} \frac{i\omega\alpha\gamma_w}{G\lambda^2} \tag{66}$$

$$C_3 = \lambda_* + c' - 1 \tag{67}$$

In Figures 6 and 7, the sensitivity curves are presented. We find that the largest sensitivity occurs at a certain depth in the sediment. Beyond this depth, the sensitivity decreases rapidly. As mentioned in the above section, the pore pressure is sensitive to porosity for small porosity (Figure 6), but the influence depth is shallower (see Figure 4 left diagram). Figure 7 represents the pore pressure sensitivity to degree of saturation. The curves indicate that the pore pressure sensitivity decreases with the degree of saturation. It reveals that the pore pressure has the largest variation as the sediment varies from fully saturated to partially saturated condition, and with the saturation continuing to decrease, the pore pressure variation becomes smaller. Note that the imaginary part of the pore pressure represents the phase lag, hence, the right diagrams in Figures 6 and 7 basically represent the phase variation of the pore pressure. Generally, in the top few meters of the sediment, the pore pressure is sensitive to porosity and degree of saturation.

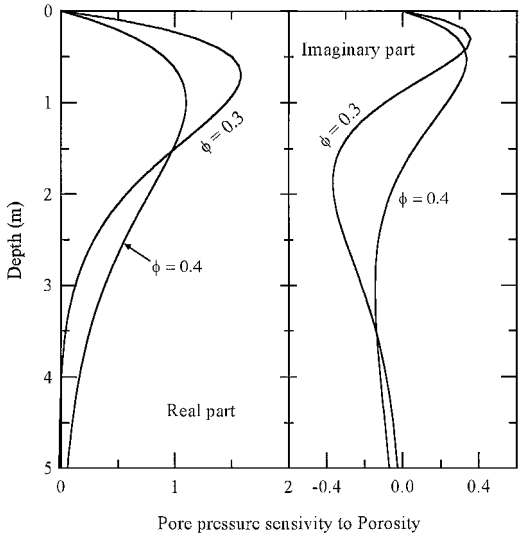


Figure 6. Pore pressure sensitivity to porosity at two different porosities

 

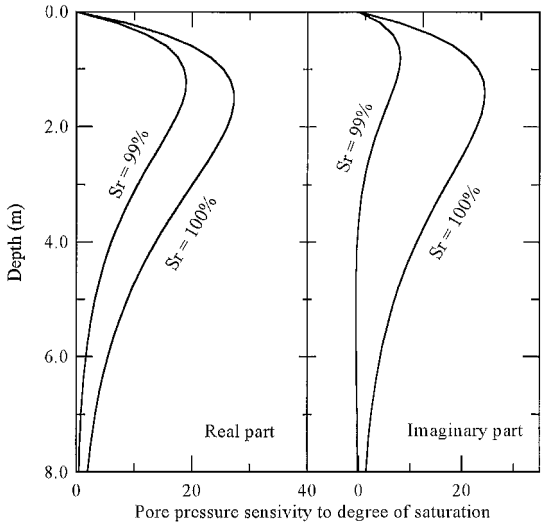


Figure 7. Pore pressure sensitivity to degree of saturation at different degree of saturation levels

Therefore, it is possible to determine the porosity and degree of saturation at the top layer of the sediment using the pore pressure data.

## 7. PARAMETER INVERSION

In the above section, we have shown that the pore pressure is sensitive to porosity and the degree of saturation at the top few metres of the sediment. In this section, a sediment parameter inversion technique is discussed. An example is presented using an artificial data set to demonstrate the feasibility of the methodology.

Assume that the measured pore water pressure at depth $z_i$ and time $t_j$ is $p^0_{i,j}$. We denote the vector $P^0_j = (p^0_{1,j}, p^0_{2,j}, \ldots, p^0_{n,j})^{\mathrm{T}}$ as the measureme nt at time $j$. At any time $j$, the model-predicted pore water pressure is expressed as $P_j$. A cost function of the parameter inversion can be defined as

$$J(\zeta_1, \zeta_2, \ldots, \zeta_m) = \sum_{j=1}^{M_t} (\overline{P_j} - \overline{P^0_j})^{\mathrm{T}} \cdot (P_j - P^0_j) \tag{68}$$

in which, $\boldsymbol{\zeta} = (\zeta_1, \zeta_2, \ldots, \zeta_m)$ is the physical parameter vector, superscript ($^{\mathrm{T}}$) stands for transpose, $M_t$ is the total number of observation time, $\overline{P_j}$ is the complex conjugate of vector $P_j$.

A homogeneous media is assumed and $\boldsymbol{\zeta} = (\phi, S_r)$ is chosen. The porosity ($\phi$) and the degree of saturation ($S_r$) will be sought by means of an optimization technique which minimizes the cost function $J(\boldsymbol{\zeta})$.

Based on the gradient method, an iteration algorithm is devised as follows:

*Step* 1. For iteration step number $n = 0$, set initial guess of the parameters $\phi^{(0)} = 0{\cdot}5$, $S_r^{(0)} = 100$ per cent.

 

*Step* 2. Solve the forward problem to obtain pore pressure $P_j$ and $\nabla_\zeta P_j$ from equations (59)–(63).
*Step* 3. Calculate the gradient matrix

$$\nabla_\zeta J(\phi^{(n)}, S_r^{(n)}) = \sum_{j=1}^{M_t} [\nabla_\zeta \overline{P_j}^{\mathrm{T}} \cdot (P_j - P_j^0) + \nabla_\zeta P_j^{\mathrm{T}} \cdot (\overline{P_j} - \overline{P_j^0})]. \tag{69}$$

*Step* 4. If $\|\nabla_\zeta J\| < \varepsilon$ (a given small number which is used to terminate the iteration), stop the iteration. $(\phi, S_r) = (\phi^{(n)}, S_r^{(n)})$ will be the optimized parameter vector. Otherwise, go to Step 5.
*Step* 5. Ajust parameters from the following equation:

$$\begin{pmatrix} \phi^{(n+1)} \\ S_r^{(n+1)} \end{pmatrix} = \begin{pmatrix} \phi^{(n)} \\ S_r^{(n)} \end{pmatrix} - \theta \nabla_\zeta J(\phi^{(n)}, S_r^{(n)}) \tag{70}$$

where $\theta$ $(0 < \theta < 1)$ is a step factor. An alternative way to find the $\theta$ can be an arbitrary guess based on experience, or, more systematically, found from Hessen matrix, which leads to the Gauss–Newton method.
*Step* 6. Update the initial guess (set $n + 1 \to n$) and go to Step 2.

To test the inverse method, an example is presented. Using value of 0·40 and 0·99, respectively, for porosity and degree of saturation, an artificial data set is generated from the forward solution. For the water wave input parameters, we take into consideration that the real ocean waves are not of a single frequency. In the present test, we assume that the input water wave consists of three major frequency components of 0·12, 0·17 and 0·24 Hz, with an energy partition that leads to the wave heights of 0·18, 0·65 and 0·26 m, respectively. This synthesized data set are calculated from the forward solution. The data set at the mud line is presented in Figure 8, as three single waves,

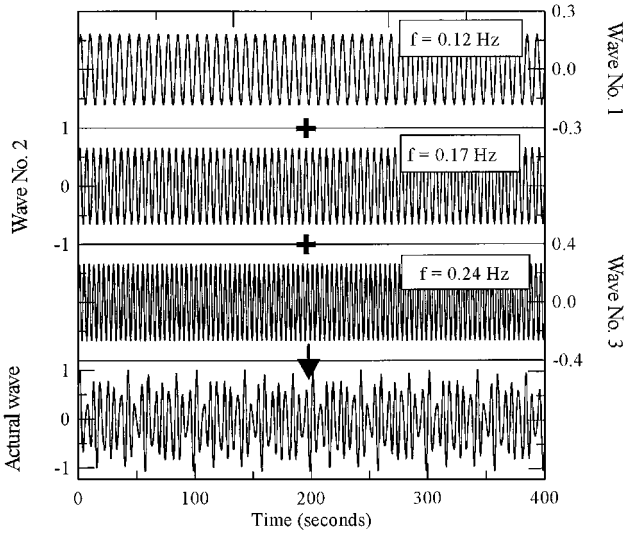


Figure 8. Artificial water wave profile. Three frequency waves generate the total wave which acts onto the sediment

 

Table I. Inversion results of the porosity and degree of saturation with both exact data input and data input containing random errors

| Parameters | The exact parameters | Inversion results | |
|---|---|---|---|
| | | With exact data input | With random errors input |
| $\phi$ | 0·4000 | 0·4000 | 0·4073 |
| $S_r$ | 0·9900 | 0·9901 | 0·9907 |

and as the superposition. A random error of 10 per cent of the data is also introduced into the synthetic data to represent the white noise which may exist in the real data.

Since the forward solution is a single frequency solution, in reality, the experimental data need to be decomposed into multiple single frequency waves. With the introduction of the multiple single frequency waves in the water column, the cost function for the parameter inversion can be modified as

$$J = \sum_{i=1}^{N_f} J_{f_i} \tag{71}$$

in which, $N_f$ is the total number of single waves extracted from the water wave, $f_i$ is the frequency of the $i$th wave component.

The investigation of the parameter inversion follows the above proposed procedures. The inverted parameters for this example are listed in Table I.

From this example, we found that the inversion method is reliable and accurate. Even with an amount of random noise, the parameter inversion is still satisfactory. With the empirical relationships presented above, other sediment physical parameters, such as shear modulus, frame bulk modulus and permeability can be estimated from the porosity.[11]

## 8. CONCLUSION

In this paper, we have presented an analytical solution for the evaluation of seepage flux exchange between the ocean and the ocean sediment under the action of water waves. The results show that under the assumption of fully saturated sediment, the Darcy's law based theory provides an excellent prediction of seepage flux. The relations show linear dependence of water flux to hydraulic conductivity. They also show that water flux is inversely proportional to water weave frequencies. The results also demonstrate that when the degree of saturation is slightly less than 100 per cent, the predicted exchange flux significantly deviates from Darcy's law based theory. The volume becomes strongly dependent on many parameters, including anisotropy in hydraulic conductivity, porosity, shear modulus of the sediment, etc.

Next, the physical parameter effects on the pore pressure are analysed. Analytical formulas of the pore pressure sensitivity to sediment parameters are presented for homogeneous isotropic sediment. Recognizing that the pore pressure is sensitive to a few of the basic sediment parameters, a parameter inversion technique is proposed. Using a set of artificially generated data set with random noise, it is demonstrated that the inverse algorithm can accurately determine the physical parameters.

 

## ACKNOWLEDGEMENTS

This research was partially supported by the Office of Naval Research.

## APPENDIX

*Solutions of the 6 × 6 matrix equations*

*Case* 1: Ocean has a porous sediment with thickness of $h$ m laying on an impermeable basement. The boundary conditions (11)–(13) and (15)–(17) are satisfied. By submitting of expressions (22)–(24) into these 6 boundary conditions, a $6\times6$ matrix equation system is constructed as

$$\begin{bmatrix} 2\lambda & 0 & 0 & 1-\lambda A_1 & 2\lambda' & 0 \\ 0 & 1-\lambda A_1 & \frac{1-2v}{1-v}\lambda & 0 & 0 & \lambda(\lambda_*^2-\frac{v}{1-v}) \\ 0 & A_2 & 0 & 0 & 0 & -A_3 \\ \mathrm{sh}(\lambda d) & d\,\mathrm{sh}(\lambda d) & \mathrm{ch}(\lambda d) & d\,\mathrm{ch}(\lambda d) & \mathrm{sh}(\lambda' d) & \mathrm{ch}(\lambda' d) \\ \mathrm{ch}(\lambda d) & F_1 & \mathrm{sh}(\lambda d) & F_2 & \lambda_*\mathrm{ch}(\lambda' d) & \lambda_*\mathrm{sh}(\lambda' d) \\ 0 & \mathrm{sh}(\lambda d) & 0 & -\mathrm{ch}(\lambda d) & \frac{A_3\lambda_*}{A_2}\mathrm{ch}(\lambda' d) & \frac{A_3\lambda_*}{A_2}\mathrm{sh}(\lambda' d) \end{bmatrix} \begin{Bmatrix} a_1 \\ a_2 \\ a_3 \\ a_4 \\ a_5 \\ a_6 \end{Bmatrix} = \begin{Bmatrix} 0 \\ b \\ 1 \\ 0 \\ 0 \\ 0 \end{Bmatrix} \tag{72}$$

in which, the parameters involved were the same as explained in the text and

$$\mathrm{sh}(x) = (\mathrm{e}^x - \mathrm{e}^{-x})/2 \tag{73}$$

$$\mathrm{ch}(x) = (\mathrm{e}^x + \mathrm{e}^{-x})/2 \tag{74}$$

$$F_1 = d\,\mathrm{ch}(\lambda d) - A_1\,\mathrm{sh}(\lambda d) \tag{75}$$

$$F_2 = d\,\mathrm{sh}(\lambda d) - A_1\,\mathrm{ch}(\lambda d) \tag{76}$$

$$b = (\alpha - 1)(1-2v)/2(1-v) \tag{77}$$

Solving these equations, we have

$$a_1 = -\frac{1-\lambda A_1}{2\lambda}a_4 - \lambda_* a_5 \tag{78}$$

$$a_2 = \frac{1}{A_2} + \frac{A_3}{A_2}a_6 \tag{79}$$

$$a_3 = \frac{1-v}{1-2v}\left(\frac{bA_2 + \lambda A_1 - 1}{A_2\lambda} - \frac{F_3}{\lambda}a_6\right) \tag{80}$$

and

$$a_4 = \begin{vmatrix} b_1 & a_{12} & a_{13} \\ b_2 & a_{22} & a_{23} \\ b_3 & a_{32} & a_{33} \end{vmatrix} \Big/ B \tag{81}$$

 

$$a_5 = \begin{vmatrix} a_{11} & b_1 & a_{13} \\ a_{21} & b_2 & a_{23} \\ a_{31} & b_3 & a_{33} \end{vmatrix} \Big/ B \tag{82}$$

$$a_6 = \begin{vmatrix} a_{11} & a_{12} & b_1 \\ a_{21} & a_{22} & b_2 \\ a_{31} & a_{32} & b_3 \end{vmatrix} \Big/ B \tag{83}$$

$$B = \begin{vmatrix} a_{11} & a_{12} & a_{13} \\ a_{21} & a_{22} & a_{23} \\ a_{31} & a_{32} & a_{33} \end{vmatrix} \tag{84}$$

in which

$$a_{11} = \frac{\lambda A_1 - 1}{2\lambda} \operatorname{sh} \lambda d + d \operatorname{ch} \lambda d \tag{85}$$

$$a_{12} = -\lambda_* \operatorname{sh} \lambda d + \operatorname{ch} \lambda' d \tag{86}$$

$$a_{13} = \operatorname{ch} \lambda' d + \frac{d A_3}{A_2} \operatorname{sh} \lambda d - \frac{(1-v)F_3}{(1-2v)\lambda} \operatorname{ch} \lambda d \tag{87}$$

$$a_{21} = \frac{\lambda A_1 - 1}{2\lambda} \operatorname{ch} \lambda d + F_1 \tag{88}$$

$$a_{22} = -\lambda_* \operatorname{ch} \lambda d + \lambda_* \operatorname{ch} \lambda' d \tag{89}$$

$$a_{23} = \lambda_* \operatorname{sh} \lambda' d + \frac{A_3}{A_2} F_1 - \frac{(1-v)F_3}{(1-2v)\lambda} \operatorname{sh} \lambda d \tag{90}$$

$$a_{31} = -\operatorname{ch} \lambda d \tag{91}$$

$$a_{32} = \frac{A_3 \lambda_*}{A_2} \operatorname{ch}(\lambda' d) \tag{92}$$

$$a_{33} = \frac{A_3 \lambda_*}{A_2} \operatorname{sh}(\lambda' d) + \frac{A_3 \lambda_*}{A_2} \operatorname{sh}(\lambda d) \tag{93}$$

and

$$b_1 = -\frac{d}{A_2} \operatorname{sh} \lambda d - \frac{1-v}{1-2v} \left( \frac{b}{\lambda} - \frac{1-\lambda A_1}{\lambda A_2} \right) \operatorname{ch} \lambda d \tag{94}$$

$$b_2 = -\frac{F_1}{A_2} - \frac{1-v}{1-2v} \left( \frac{b}{\lambda} - \frac{1-\lambda A_1}{\lambda A_2} \right) \operatorname{sh} \lambda d \tag{95}$$

 

$$b_3 = -\frac{\text{sh}\,\lambda d}{A_2} \tag{96}$$

$$F_3 = \left[\lambda\left(\lambda_*^2 - \frac{v}{1-v}\right) + \frac{(1-\lambda A_1)A_3}{A_2}\right] \tag{97}$$

*Case* 2: Ocean has a semi-infinite porous sediment. Hence, boundary conditions in (18) are satisfied. Rearranging the expressions (22)–(24) into exponential format using (73) and (74), we immediately obtain

$$a_3 = -a_1 \tag{98}$$

$$a_4 = -a_2 \tag{99}$$

$$a_6 = -a_5 \tag{100}$$

Hence, the unknowns reduce to only three, $a_1, a_2$ and $a_5$. They can be easily solved from boundary conditions (11)–(13). In expressions of $C_1, C_2$ and $c'$ defined in the text part, we have

$$a_1 = \frac{A_1 C_2 - A_1 C_1 c'}{2A_2 C_2} + \frac{\lambda_* C_1 c'}{A_3 C_2} \tag{101}$$

$$a_2 = \frac{C_2 - C_1 c'}{A_2 C_2} \tag{102}$$

$$a_5 = \frac{C_1 c'}{A_3 C_2} \tag{103}$$

## REFERENCES


1. P. L. F. Liu, 'Damping of water waves over porous bed', *J. Hydraul. Div., Am. Soc. Civ. Engng., ASCE*, **99**(HY12). 2263–2271 (1973).
2. W. W. Mallaid and R. A. Dalrymple, 'Water waves propagating over a deformable bottom', *Offshore Tech. Conf.*, OTC 2895, Houston, Texas, 1977.
3. S. R. Massel, 'Gravity waves propagated over permeable bottom', *J. WHCE, ASCE*, **102**(WW2)**,** 111–121 (1976).
4. H. Moshagen and A. Torum, 'Wave induced pressures in permeable seabeds', *J. WHCE, ASCE*, **101**(WW1)**,** (1975).
5. M. Badiey, I. Jaya, W. Magda and W. Richwien, 'Analytical and experimental approach in modeling of water-seabed interaction', *Proc. 2nd Int. Offshore and Polar Engng. Conf.*, 1992, pp. 398–402.
6. O. S. Madsen, 'Wave-induced pore pressures and effective stresses in a porous bed, *Geotechnique*, **29,** 377–393 (1978).
7. T. Yamamoto, 'On the response of poro-elastic bed to water waves', *J. Fluid Mech.*, **87**(Part 1)**,** 193–206 (1978).
8. Mei and Foda, 'Wave-induced response in a fluid-filled poro-elastic solid with a free surface: a boundary layer theory', *Geophys. J. Roy. Astrong*, **66,** 597–631 (1981).
9. M. A. Biot, 'General theory of three-dimensional consolidation', *J. Appl. Phys.*, **12,** 155–164 (1941).
10. R. H. Bennett, J. T. Burns, H. Li, D. J. Walter, P. J. Valent, C. M. Percival and J. Lipkin, 'Subseabed disposal project experiment: Piezometer probe measurement technology', in K. Demars and R. Chaney (eds), *Geotechnical Engineering of Ocean Waste Disposal*, ASTM STP 1087, 1990, p. 175.
11. M. Badiey, A. H.-D. Cheng and Y. Mu, 'From geology to geoacoustics—Evaluation of Biot-Stoll sound speed and attenuation for shallow water acoustics', *J. Acoust. Soc. Am.*, **103,** 309–320 (1998).
12. E. Detournay and H.-D. A. Cheng, 'Fundamentals of poroelasticity', in (ed.), C. Fairhurst *Principles, Practice and Projects*, **II**, *Analysis Design Method*, Pergamon Press, Oxford, 1993.
13. Y. Mu, 'Response of poroelastic seabed to acoustic and water waves', *Ph.D. Thesis*, University of Delaware, May 1998.
14. P. C. Carman, *Flow of Gases Through Porous Media*, Academic Press, New York, 1956.


 

15. T. Yamamoto, Trevorrow, M. Badiey and A. Turgut, 'Determination of the seabed porosity and shear modulus profiles using a gravity wave inversion', *Geophys. J. Int*., **98,** 173–182 (1989).
16. T. W. Lambe and R. V. Whitman, *Soil Mechanics*, Wiley, New York, 1969.
17. E. L. Hamilton, 'Elastic properties of marine sediments', *J. Geophys. Res*., **76,** 579–604 (1971).
18. R. Stoll and T. K. Kan, 'Reflection of acoustic waves at a water sediment interface', *J. Acoust. Soc. Am*., **70,** 149–156 (1981).
19. A. L. Gutjahr and L. W. Gelhar, 'Stochastic models of subsurface flow: infinite versus finite domains and stationarity', *Water Resour. Res*., **17,** 337–350 (1981).
20. Y. Mu, M. Badiey and H.-D. Cheng, 'Parameter uncertainty analysis on acoustic response in fluid filled poroelastic media', *J. Acoust. Soc. Am.* (1999) submitted.

 